Experimental Evaluation of Heat Transfer Coefficient from Temperature Profiles Above the Evaporating Water Surface

Hamza Abuzienah[1], Tibor Poós[1*]

[1]Department of Building Services and Process Engineering, Faculty of Mechanical Engineering,
Budapest University of Technology and Economics, Műegyetem rkp. 3., H-1111 Budapest, Hungary

*corresponding author: poos.tibor@gpk.bme.hu

Abstract
Evaporation from open liquid surfaces is a fundamental process in many engineering applications, including cooling technologies, desalination, drying systems, and atmospheric liquid evaporation. In this context, alongside experimental measurements, curve-fitting techniques are applied to characterize the temperature distribution above the evaporating surface. This approach enables the estimation of the thermal boundary layer thickness and the determination of the heat transfer coefficient based on the resulting temperature gradient.
In this study, an experimental investigation was conducted to analyze the temperature distribution above an evaporating water surface under forced convection at bulk air temperatures of 40°C, 50°C, and 60°C. The air flows over the open water surface at a controlled velocity of 1.5 m/s. The temperature field above the liquid surface was measured using multiple thermocouples positioned at different vertical distances from the interface. In addition, supplementary measurements were conducted to determine the surface temperature, bulk air temperature, and ambient humidity conditions. By using the measured temperature profile, the heat transfer coefficient was evaluated from the temperature gradient at the surface. The results of this study also showed that the heat transfer coefficient is higher than Nusselt correlation and decreases as the thermal boundary layer thickness increases, which is consistent with classical heat transfer theory.

Keywords: Evaporation; Temperature profile; Heat transfer coefficient; Forced convection.

Nomenclature

$\dot{q}$	Heat flux, W/m^2
T	Temperature of bulk air, $°C$
z	Distance above the water surface, m
c	Specific heat, $J/kg\ K$
v	Velocity of air, m/s
a, m	Constant
Greek Symbols	
λ	Thermal conductivity, W/mK
δ	Boundary layer, mm
α	Heat transfer coefficient, W/m^2K
ρ	Density of air, kg/m^3
β	Properties constant
Non-dimensional Numbers	
Nu	Nusselt number, $\alpha L/\lambda$
Re	Reynolds number, $\rho v L/\mu$
Pr	Prandtl number, $c_p \mu/\lambda$
Gu	Gukhman number, $(T_G - T_f)/(T_G + 273.15)$
Subscripts	
t	Thermal
G	Bulk gas
f	Water surface
$conv$	Convection
z	Direction of flow

1. Introduction

A vapor pressure differential between the liquid surface and the bulk air causes molecules to escape from the liquid phase into the surrounding gas during evaporation from an open liquid surface, a coupled heat- and mass-transfer process. Many industrial and environmental applications, including drying, cooling systems, and building energy processes, depend heavily on this phenomenon [1]. To provide the latent heat needed for phase shift during evaporation, heat must be applied to the liquid's surface. Consequently, convection and conduction transfer heat from the surrounding air to the liquid-contact surface. The magnitude of this heat transfer, which relates the heat flux to the temperature difference between the liquid surface and the surrounding air, is typically characterized by the convective heat transfer coefficient. This coefficient depends on several factors, such as air velocity, fluid characteristics, temperature differential, and flow regime laminar or turbulent, according to classical heat transfer theory [2]. A thermal boundary layer is created by the temperature field in the gas region above the liquid surface, where temperature changes with vertical distance from the interface. The equilibrium between convective mixing and conductive heat transport in the gas phase is reflected in the temperature profile in this area. Temperature gradients within this boundary layer control the rate of heat transfer to the evaporating surface, which in turn significantly affects the evaporation rate, according to transport studies [3]. The Nusselt correlation for non-heating water with a turbulent air stream in a range of $Re \cong [3 \cdot 10^5 - 16 \cdot 10^5]$, and flowing over a free water surface can be obtained by Nusselt correlation as follows [4]:

$$Nu = 0.083\, Re^{2/3} Pr^{1/3} Gu^{0.1} \tag{1}$$

Therefore, precise estimation of heat transfer coefficients and thermal boundary thickness requires an understanding of the temperature distribution above the liquid surface.

This work aims to determine temperature profiles experimentally and represented by an exponential model to determine the convective heat transfer coefficient experimentally (α_{conv}) for different gas temperatures.

2. Methodology

The temperature distribution in the air region above an evaporating water surface under forced-convection conditions was examined using an experimental setup. A regulated convective flow was created by forcing air across the water's surface at a velocity of $1.5\ m/s$. Type-T thermocouples placed at vertical distances of $1\ mm$, $3\ mm$, $7\ mm$, and $15\ mm$ above the liquid interface were used to measure the temperature profile within the gas phase. These observations provide the temperature gradient needed to calculate the heat transfer coefficient and enable the characterization of the thermal boundary layer that forms above the evaporating surface. The temperature gradient in the thermal boundary layer above the liquid surface can be used to calculate the heat transfer coefficient. The temperature profile can determined from the energy equation as follows [2]:

$$\rho c_p v_z \frac{dT}{dz} = \lambda_G \frac{\partial^2 T}{\partial z^2} \tag{2}$$

Fourier's law of heat conduction at the interface, when conduction is the primary mode of heat transmission, can be used to determine the local surface heat flow, according to classical heat transfer theory. Thus, the surface heat flux can be written as [2]:

$$\dot{q} = -\lambda_G \left(\frac{dT}{dz}\right) \tag{3}$$

Newton's law of cooling can also be used to express the same heat flow in convective heat transfer [2]:

$$\dot{q} = \alpha_{conv}(T_f - T_G) \tag{4}$$

All properties are constant, and $\beta \cong \rho c_p v_z$, and rearrange Eq. (2) as follows:

$$\frac{\partial^2 T}{\partial z^2} - \frac{\beta}{\lambda_G}\frac{dT}{dz} = 0 \tag{5}$$

Solving this equation into ODE by reduction the order, and assuming that $T = e^{mz}$, $a = \frac{\beta}{\lambda_G}$, and make a substitution simplify the equation:

$$m^2 e^{mz} - a m e^{mz} = 0 \tag{6}$$

Now rearrange the equation to get the simplify for m:

$$m^2 - am = 0 \rightarrow m\,(m - a) = 0 \tag{7}$$

The values of m for solving this equation:

$$m = 0\,, m = a \tag{8}$$

The final solution of T:

$$T(z) = C_1 + C_2 e^{az} \tag{9}$$

Now we apply the boundary condition to get C_1, C_2 values when $z = 0\,, T = T_f$ and $z = \infty\,, T = T_G$, but when $a > 0$, $\mathrm{e}^{az} = \infty$ so $\beta > 0$, and $a = -\beta$ as follows:

$$T(\infty) = T_G = C_1 + C_2 e^{-(\infty)z} \rightarrow C_1 = T_G \tag{10}$$

And:

$$T(0) = T_f = C_1 + C_2 e^{-(0)z} \rightarrow C_2 = T_f - T_G \tag{11}$$

Then the Temperature profile equation:

$$T(z) = T_G + (T_f - T_G)e^{-az} \tag{12}$$

Applying temperature profile model for Fourier's law, get:

$$\dot{\mathrm{q}} = -\lambda_\mathrm{G}\left(\frac{\mathrm{dT}}{\mathrm{dz}}\right) = -\lambda_\mathrm{G}\,(-a(\mathrm{T_f} - \mathrm{T_G})\mathrm{e}^{-az}) \tag{13}$$

So, the heat flux from Fourier's law at the surface ($\mathrm{z} = 0$):

$$\dot{\mathrm{q}} = \lambda_\mathrm{G} a(\mathrm{T_f} - \mathrm{T_G}) \tag{14}$$

When equaled Eq. (14) with Newton's Law as follows:

$$\lambda_G a\left(T_f - T_G\right) = \alpha_{conv}(T_f - T_G) \tag{15}$$

Then the resulting equation:

$$a = \frac{\alpha_{conv}}{\lambda_G} \cong \frac{\beta}{\lambda_G} \cong \frac{\rho c_p v_z}{\lambda_G} \tag{16}$$

From Fourier's law equated Newton cooling law, we determine the calculation method of heat transfer coefficient as shown:

$$\alpha_{conv} = \frac{-\lambda_G\left(\frac{dT}{dz}\right)_{z=0}}{(T_f - T_G)} \tag{17}$$

Determination of the thermal conductivity for the air by following the relation [5]:

$$\lambda_G = \frac{C_1 {T_G}^{C_2}}{1 + \frac{C_3}{T_G} + \frac{C_4}{{T_G}^2}} \tag{18}$$

Where $C_1 = 0.00031417;\ C_2 = 0.7786;\ C_3 = -0.7116;\ C_4 = -0.7116$.

To determine the a, from Eq. (12) we arrange it to get the dimensionless temperature, as follows:

$$\theta = \frac{\mathrm{T(z)} - \mathrm{T_G}}{\mathrm{T_f} - \mathrm{T_G}} = \mathrm{e}^{-az} \tag{19}$$

The range of θ is 1 at T_f and 0 at T_G, solving for z to get a linear relation with θ:

$$ln\,\theta = ln\,e^{-az} \rightarrow ln\,\theta = -az \tag{20}$$

The measured temperature data were processed using MATLAB, where curve fitting was applied to improve a continuous temperature profile and estimate the temperature gradient near the surface [6].

3. Results and Discussion

The measured temperature increases with distance from the water surface, indicating the presence of a thermal boundary layer above the evaporating interface. Using measured temperatures at different positions, the temperature gradient near the surface was estimated and used to calculate the heat transfer coefficient. The results show that heat transfer near the interface is mainly governed by conduction within the thermal boundary layer under the imposed airflow of $1.5\ \mathrm{m/s}$ with the relative humidity of the ambient air $[24 - 34\%]$, and different air temperatures.

Figure 1 shows the temperature profile above the water surface for different air temperatures T_G=40; 50; 60°C. The temperature increases with distance from the surface, indicating the presence of a thermal boundary layer. A strong temperature gradient is observed near the interface due to evaporation and the wet layer.

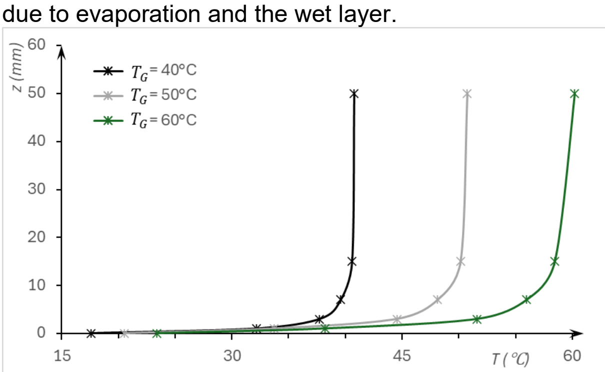

Fig. 1. Temperature profiles above the water surface for $T_G = 40;\ 50;\ 60°C$

Figure 2 shows the difference between the temperature profile method and the Nusselt correlation method. This method yields higher results because it's more accurate than the Nusselt correlation at the surface during evaporation.

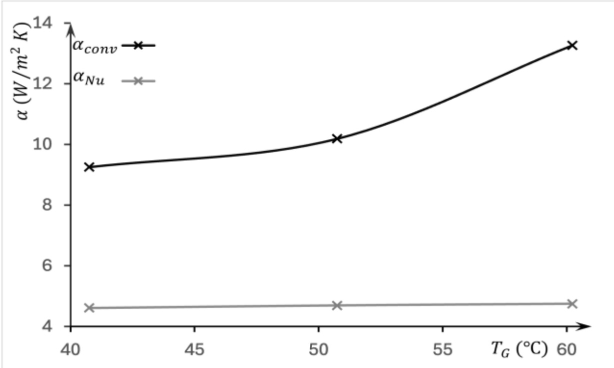

Fig. 2. Heat transfer coefficient by temperature profile method and Nusselt correlation

Overall, the measured temperature profiles confirm the formation of a thermal boundary layer above the evaporating surface, and the calculated heat transfer coefficient shows a clear inverse relationship with the thermal boundary layer.

Measured temperature profiles and experimental findings, including the thermal boundary layer and heat transfer coefficient in each scenario, are shown in Table 1.

Table 1: Experimental temperature profiles and heat transfer coefficient for different cases

#	T_G	T_f	δ_t	α_{conv}	Nu	α_{Nu}	$\Delta\alpha = \lvert\alpha_{conv} - \alpha_{Nu}\rvert$	$\delta\alpha = \frac{\Delta\alpha}{\alpha_{conv}}$
	$[°C]$	$[°C]$	$[mm]$	$[W/m^2\ K]$	$[1]$	$[W/m^2\ K]$	$[W/m^2\ K]$	[%]
1	40.8	17.6	2.840	9.25	52.8	4.61	4.64	50
2	50.8	20.5	2.625	10.19	52.8	4.69	5.49	54
3	60.2	23.4	2.049	13.26	52.5	4.74	8.51	64

3. Conclusion

The experimental temperature profiles displayed a clear exponential pattern, indicating a well-defined thermal boundary layer above the evaporating surface. Heat transfer coefficient by temperature profiles gets higher values than Nusselt correlation. The calculated heat transfer coefficient showed an inverse relationship with the thermal boundary layer thickness, consistent with $\boldsymbol{\alpha_{conv}\sim 1/\delta_t}$, where thicker boundary layers led to lower $\boldsymbol{\alpha_{conv}}$ values. Variations between cases were primarily due to differences in operating conditions and temperature levels, which influence both boundary layer development and air thermal conductivity. Temperature profile method is accurate at the surface and sensitive, and it improves in the determination of $\boldsymbol{\delta_t}$ and $\boldsymbol{\alpha_{conv}}$. Overall, the results confirm that the temperature profile is an effective and practical method for evaluating thermal boundary layers and heat transfer coefficients in open surface evaporation systems, providing physically consistent and reliable insights under diverse experimental conditions.

Funding

This work was supported by the János Bolyai Research Scholarship of the Hungarian Academy of Sciences (BO/00059/23/6) and by the Hungarian Scientific Research Fund (NKFIH FK-14220).

References

[1] W. K. Lewis, "The Evaporation of a Liquid Into a Gas," *Trans. Am. Soc. Mech. Eng.*, vol. 44, pp. 325–332, Jan. 1922, doi: 10.1115/1.4058175.

[2] F. P. Incropera, D. P. DeWitt, T. L. Bergman, and A. S. Lavine, Eds., *Fundamentals of heat and mass transfer*, 6. ed. Hoboken, NJ: Wiley, 2007.

[3] R. B. Bird, W. E. Stewart, and E. N. Lightfoot, *Transport phenomena*, 2nd, Wiley international ed ed. New York: J. Wiley, 2002.

[4] B. M. Smolsky and G. T. Sergeyev, "Heat and mass transfer with liquid evaporation," *Int. J. Heat Mass Transf.*, vol. 5, no. 10, pp. 1011–1021, Oct. 1962, doi: 10.1016/0017-9310(62)90081-9.

[5] D. W. Green and M. Z. Southard, *Perry's Chemical Engineers' Handbook, 9th Edition*, 9th edition. New York, N.Y: McGraw-Hill Education, 2019.

[6] *MATLAB*. (2024). MathWorks, Natick, MA, USA.